

## Study of the vibrational modes of GaSb/AlSb (001) superlattices

D. Berdekas\*

*Direction of Education of High Schools of Larissa, Lykeio Abelona, 40400 Larissa, Hellas.*

*Received 16 April 2008; Accepted 23 February 2009*

---

### Abstract

In the present work, we study the modes of vibration of small period (GaSb)<sub>n</sub>/(AlSb)<sub>n</sub> superlattices, n=1,2,3, grown along (001) direction. Any superlattice (SL) is described by a three dimensional elementary cell several times bigger of the elementary cell of the zinc blend bulk constituents. The modes of vibration are calculated using a ten parameter (10) Valence Overlap Shell Model, with the interactions of the binaries GaSb and AlSb calculated with different parameter sets, for both short and long range forces. With the atomic displacements known, we calculated the Raman spectra, away of resonance conditions, based on the Bond Polarizability Model. Our results are in good agreement with the existing experimental data.

*Keywords:* Superlattices, Lattice Dynamics, Raman scattering, phonons.

---

### 1. Introduction

In contrast to the big amount of studies on GaAs/AlAs SLs, only a relatively small number of works on GaSb/AlSb SLs exist, focused mainly on the electronic properties [1],[2]. The dynamical properties have not been studied theoretically up to now, while only two experimental studies exist, tracing by the means of the Raman scattering technique, some of the lattice vibrations of these materials [3],[4].

The so restricted information on the dynamical properties of these materials was the motive for this work, which is organized in the following way. Firstly, based on a ten (10) parameter Valence Overlap Shell Model [5],[6] we calculated, the phonon dispersion curves for both bulk GaSb and AlSb crystals. The calculation of the interactions between the atoms is made with different parameter sets for each one of the constituents. Next, we construct the dynamical matrix for each SL, properly combining the elements of the dynamical matrices of the GaSb and AlSb. we present the calculated phonon dispersion curves for GaSb/AlSb SLs (001) for certain high symmetry directions.

In the final step, we present Raman spectra calculations for the longitudinal modes of vibration in the long wavelength limit with wave vector propagating along the growth direction for the three cases (n = 1, 2, 3). The calculations are accomplished with the Bond Polarizability Model [7]. The results are in good agreement with the experimental data.

### 2. Phonon calculations of the bulk constituents

The calculation of the atomic force constants for each material,

according to the Valence Overlap Shell Model (VOSM) [5],[6], presumes the knowledge of the values of the ten parameters the model employs. These parameters are which describe the long-range interactions, the next two are the core-shell coupling parameters. The  $\epsilon$   $Z$ ,  $Y_1$ ,  $Y_2$ ,  $k_1$ ,  $k_2$ ,  $\lambda$ ,  $k_{r10}$ ,  $k'_{r10}$ ,  $k_{r20}$ ,  $k'_{r20}$ . The first three are the electric parameters last five ones are the valence-force-field parameters, which describe the short-range interactions. The values of the model parameters are obtained by a least-squares fitting procedure of the calculated phonon frequencies to the experimentally known phonon dispersion of the bulk compounds GaSb and AlSb. The aim of this procedure is to find the proper minimum based on the relation

$$\chi^2 = \sum (\omega_{\text{calc}} - \omega_{\text{exp}})^2 \quad (1)$$

From the fitting procedure for the GaSb crystal, we found the following parameter set :  $Z= 2$ ,  $Y_1= 4.941$ ,  $Y_2= 3.56$ , (proton charges)  $k_1= 17.19$ ,  $k_2= 4.346$ ,  $\lambda= 1.732$ ,  $k_{r10}= 0.176$ ,  $k'_{r10}= -0.183$ ,  $k_{r20}= -0.0435$ ,  $k'_{r20}= - 0.0054$  (in  $10^5$  dyn/cm units). The mean standard deviation is  $3.5 \text{ cm}^{-1}$  per phonon. The values of the elastic constants obtained by this parameter set are (in parenthesis the experimental ones)  $C_{11}= 8.6$  (8.9),  $C_{12}= 4.7$  (4.0),  $C_{44}= 3.5$  (4.3) (in  $10^{11}$  dyn/cm<sup>2</sup> units).

In Fig. 1 is shown the phonon dispersion curves of the bulk GaSb crystal in the high symmetry directions X,  $\Sigma$ , L, X-W. The boxes are the experimental frequencies. Except from the middle of the higher frequency acoustic branch along  $\Sigma$  direction the overall fitting is very good.

In Fig. 2 it is shown the one phonon density of states of GaSb. The frequencies are calculated using a uniform mesh in the irreducible part of the 1<sup>st</sup> Brillouin using weighting factors. As

---

\* E-mail address: dberdek@sch.gr

expected the distribution of the vibrational modes is much more dense in the optic frequency range where the bandwidth of the modes is much more narrow from the acoustic range.

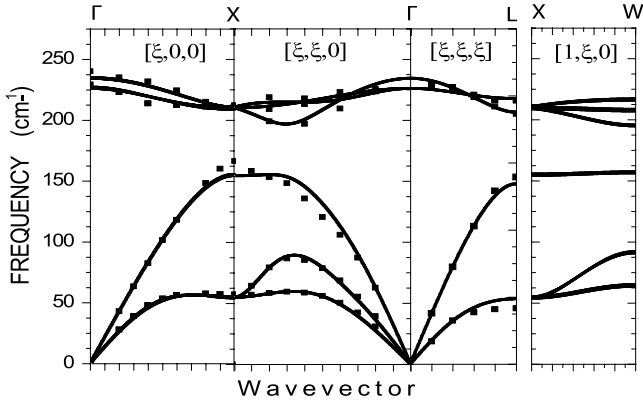


Figure 1. Phonon dispersion curves for GaSb

From the fitting procedure for the AlSb crystal, we found the following parameter set :  $Z = 2$ ,  $Y_1 = 5.131$ ,  $Y_2 = 3.742$ , (in proton charges)  $k_1 = 14.89$ ,  $k_2 = 5.71$ ,  $\lambda = 1.762$ ,  $k_{r1\theta} = 0.206$ ,  $k'_{r1\theta} = -0.166$ ,  $k_{r2\theta} = -0.066$ ,  $k'_{r2\theta} = 0.0125$  (in  $10^5$  dyn/cm units). The mean standard deviation is  $5.2 \text{ cm}^{-1}$  per phonon. The values of the elastic constants obtained by this parameter set are (in parenthesis the experimental ones)  $C_{11} = 8.6$  (8.8),  $C_{12} = 5.2$  (4.40),  $C_{44} = 3.3$  (4.0) (in units  $10^{11} \text{ dyn/cm}^2$ ).

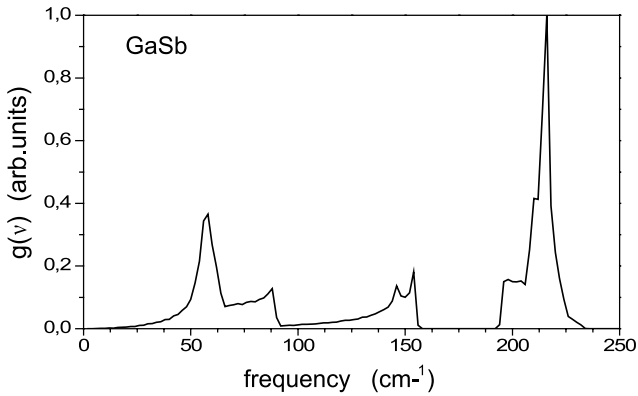


Figure 2. One phonon density of states of GaSb

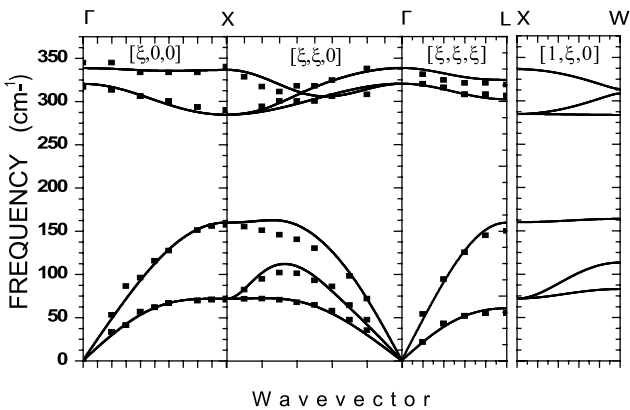


Figure 3. Phonon dispersion curves for AlSb

In Fig. 3 is shown the phonon dispersion curves of the bulk AlSb crystal in the high symmetry directions X,  $\Sigma$ , L, X-W. The boxes are the experimental frequencies. The deviation between theoretical and experimental values is considerably larger than that of GaSb because, in AlSb, apart from  $\Sigma$  direction, see Fig. 3, even  $\Delta$  direction, usually the most easy to be adjusted, introduces not negligible deviations from the corresponding experimental values. Also the LO( $\Lambda$ ) branch introduces deviations from experiment.

In Fig. 4 it is shown the one phonon density of states of AlSb, calculated in the same way as for GaSb. In this case the distribution of the vibrational modes is also more dense in the optic frequency range, but with a larger bandwidth, than that of GaSb.

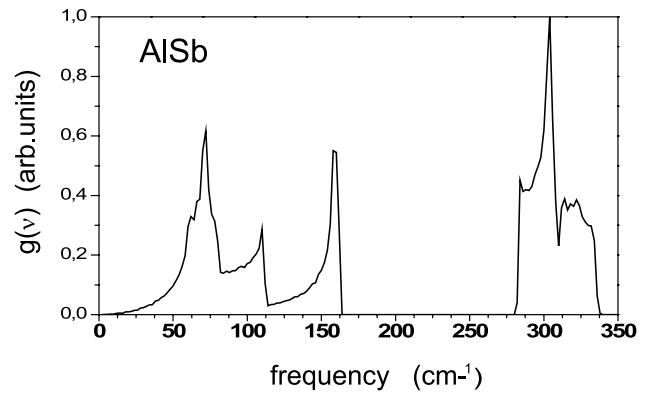


Figure 2. One phonon density of states of AlSb

### 3. Superlattice phonon calculations

For the construction of the dynamical matrix for any SL, we use a method according to which the dynamical matrix of the SL is obtained from the dynamical matrices of the bulk constituents [6],[8]. For this purpose, we define a new unit cell, from now on supercell, N times bigger the zinc blend primitive cell. This supercell is chosen to have the same translation vectors with the SLs primitive cell. Next, the dynamical matrix for each bulk constituent is calculated using the supercell in the following way. We construct a  $6N \times 6N$  block diagonal matrix with N blocks along its main diagonal. Each  $6 \times 6$  block contains a  $6 \times 6$  dynamical matrix of the bulk constituent calculated at the points of the original Brillouin zone which are folded to the center of the new Brillouin zone. For example, in  $1 \times 1$  SL case, for a given wave vector  $y$ , we construct a  $12 \times 12$  block diagonal matrix  $D^o$ .

$$D^o(y) = \begin{pmatrix} D(y) & 0 \\ 0 & D(\mathbf{b}_z + y) \end{pmatrix} \quad (2)$$

$$D^s(y) = G D^o(y) G^{-1} \quad (3)$$

$D(y)$ ,  $D(\mathbf{b}_z + y)$  are  $6 \times 6$  matrices calculated using the original elementary cell, and  $\mathbf{b}_z = (0, 0, 1) (2\pi/a)$  is the point of the original Brillouin zone (zinc blend) which is folded to the center of the new Brillouin zone of  $1 \times 1$  SL.

By a similarity transformation, we obtain the new dynamical matrix of the bulk constituent described by the new cell, supercell of the primitive zinc blend unit cell [6], [8].

With

$$G_{\alpha\beta}(\kappa\kappa',n,m) = \frac{1}{\sqrt{N_0}} \exp[2\pi i m \mathbf{b}'\mathbf{x}(\kappa,n)] \delta_{\alpha\beta} \delta_{\kappa\kappa'} \quad (4)$$

This procedure is realized for both bulk, GaSb and AlSb, constituents. Finally both 6N<sub>x</sub>6N dynamical matrices, 12x12 for 1x1 SL, are combined properly to give the SLs dynamical matrix. Care should be taken in order to be fulfilled the translation invariance condition for the SL.

In Fig. 5 it is depicted the phonon dispersion curves for the 1x1 GaSb/AlSb (001) SL for the high symmetry directions (00ξ), (ξ00), (ξ,ξ,0), (ξ'cosφ, ξ'sinφ, ξ'sinφ). Also it is shown the angular dispersion of the Γ point phonons with zero wave vector and its direction is varied from parallel to vertical to the z axis. This kind of dispersion is described by the notation (ξ'cosφ, ξ'sinφ, ξ'sinφ) with ξ' = 0. The anisotropy of the crystal with tetragonal structure is clearly demonstrated in the optic frequency range frequencies which change as the direction of the zero waves vector changes. This is Γ-θ-Γ dispersion with angle θ varying from 0 to π/2. At the Γ point, when it is approached from direction parallel to the growth direction (θ=0), the point group of the wave vector G<sub>0</sub>(k) is D<sub>2d</sub> and the modes of vibration are distributed to the irreducible representations A<sub>1</sub>+3B<sub>2</sub>+4E (A<sub>1</sub> longitudinal symmetric, B<sub>2</sub> longitudinal, E transverse). This classification is valid only in the case when all atomic interactions for both bulk are calculated with the same parameter set. The use of two different parameter sets lowers the symmetry of the SL since in GaSb layer, the force constants of Ga-Sb and Sb-Sb atoms are different from the force constants of Al-Sb and Sb-Sb atoms in the AlSb layer. So, along the (00ξ) direction the group G<sub>0</sub>(k) is C<sub>2v</sub> of the orthorhombic system and the irreducible representations of the modes of vibration are 4A<sub>1</sub>+4B<sub>1</sub>+4B<sub>2</sub> (A<sub>1</sub> symmetric longitudinal, B<sub>1</sub>, B<sub>2</sub> transverse). In the case where Γ is reached by (ξξ0) direction, the group of the wave vector G<sub>0</sub>(k) is the CS of the monoclinic system. In this case, the modes of vibration are belong to the irreducible representations 8A'+4A''. The A' modes are mixed modes with atomic displacements have components along x and z directions and the A'' modes are transverse modes with atomic displacements along y direction. Going from θ=0 [(00ξ) direction] to θ=π/2 [(ξ00) direction], due to the lowering of the symmetry, the pure longitudinal modes become mixed modes and the produced macroscopic field is decreased. As a consequence the frequencies of the A' modes are decreased. On the other hand, the branches of the A'' modes which are transverse modes with displacements along y direction are almost dispersionless, because they do not create macroscopic field. The same description holds for the phonon dispersion curves for the 2x2 SL GaSb/AlSb (001).

#### 4. Calculations of Raman Spectra

The Raman scattering intensity depends on the fourth rank tensor I<sub>αβγδ</sub> which is given by the expression [9]

$$I_{\alpha\beta\gamma\delta} = \sum_j \alpha_{\alpha\beta}(0j) \alpha_{\gamma\delta}(0j) \delta(\omega-\omega_j) [\eta(\omega_j) + 1] \quad (5)$$

α<sub>αβ</sub>(0j) the first order polarizability derivative the electronic polar-

izability with respect to the normal coordinates for the mode ω<sub>j</sub>, η(ω<sub>j</sub>) is the Bose-Einstein population factor. The function δ(ω-ω<sub>j</sub>) is approximated by the Lorentzian [9]

$$\delta(\omega-\omega_j) = \frac{1}{\pi} \frac{\Gamma_j}{[(\omega-\omega_j)^2 + \Gamma_j^2]} \quad (6)$$

where Γ<sub>j</sub> is the half width at half maximum (HWHM) of the mode j with frequency ω<sub>j</sub>.

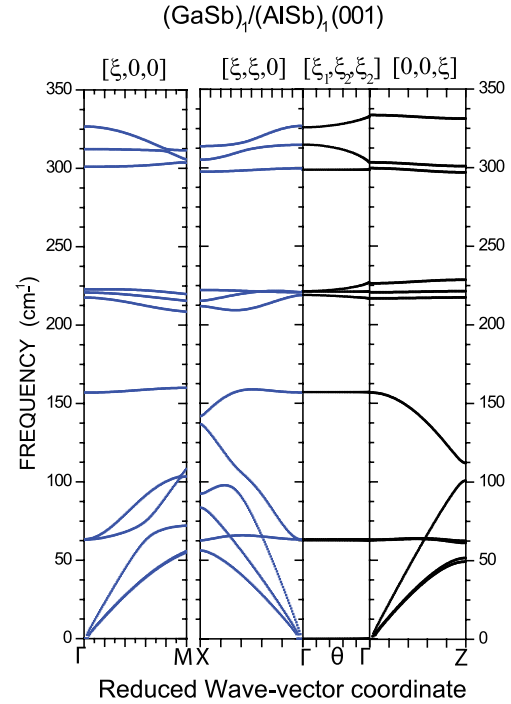


Figure 5. Phonon dispersion curves for 1X1 GaSb/AlSb (001)

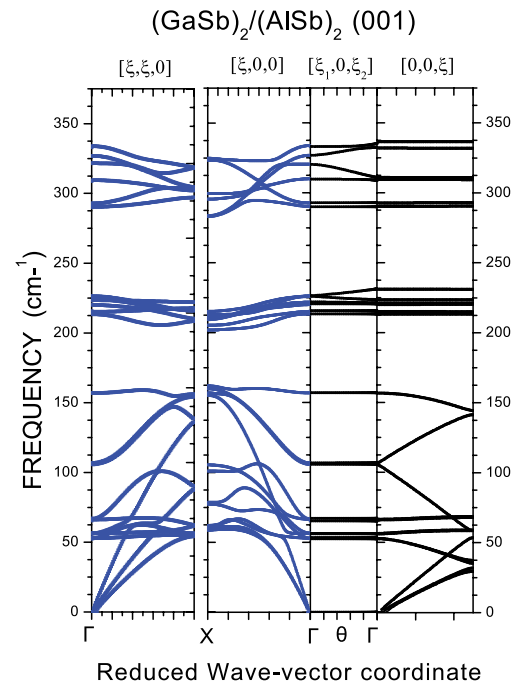


Figure 6. Phonon dispersion curves for 2X2 GaSb/AlSb (001)

The first order polarizability derivative of the electronic polarizability of the mode  $\omega_j$  with respect to the corresponding normal coordinate is given by

$$\alpha_{\alpha\beta}(0j) = \sqrt{\frac{\hbar}{\omega_j}} \sum_n \sum_\rho \left( \frac{\partial \alpha_n}{\partial \rho_\kappa} \right)_{\alpha\beta} [u_\rho(\kappa | 0j) - u_\rho(\kappa' | 0j)] \quad (7)$$

where  $n$  runs over all the bonds of the unit cell and  $\rho = x, y, z$  of the superlattice unit cell and  $u_\rho(\kappa | 0j)$  is the displacement of the atom  $\kappa$  in mode  $j$  with zero wave-vector.

The changes of the polarizability for each bond are calculated using the Bond Polarizability Model. According to this model for each bond, except the atomic displacements, are also required the parallel,  $\alpha_p$ , and vertical,  $\alpha_v$ , polarizabilities to the bond axis, along with their derivatives  $\alpha'_p$ ,  $\alpha'_v$  with respect the bond length change. The number of the unknown parameters is further reduced if we take into account the relation [10]

$$\alpha_p + 2\alpha_v = \frac{3V}{16\pi} (\epsilon_\infty - 1) \quad (8)$$

where  $V$  is the primitive cell volume of the bulk crystal and  $\epsilon_\infty$  is the high frequency dielectric constant as well the and the relation [10],

$$\alpha_p/\alpha_v = 1.1 \quad (9)$$

which holds for all III-V binaries. For simplification reasons, we made the approximation that  $\alpha_p = \alpha_v$ . Furthermore, because of the absence of adequate experimental date, based only on the fact that AlAs and AlSb have similar values for the high frequency dielectric constants, we adopted for Al-Sb bonds the values found for Al-As bonds [3]. Finally, the values we used, for the Ga-Sb (Al-Sb) bonds are  $\alpha_p = 15.0$  (6.9),  $\alpha_v = 15.0$  (6.9),  $\alpha'_p = 2.3$  (0.8),  $\alpha'_v = 0.50$  (0.50). The  $\alpha_p, \alpha_v$  are expressed in  $10^{-24} \text{ cm}^3$ , while  $\alpha'_p, \alpha'_v$  in  $10^{-16} \text{ cm}^2$  units.

In Fig. 7 are given the calculated Raman spectra away of resonance conditions for 1x1, 2x2 and 3x3 SLs GaSb/AlSb (001). All the spectra are calculated for zero wave vector propagated parallel to the layer normal, for the all the longitudinal SL modes. These modes, all of them predicted to be Raman active can be detected in the backscattering configuration  $z(x, y)z$ . Still,  $x, y, z$  coordinates refer to the zinc blend unit cell coordinates. In all three cases, the

most intense signal originates from the LO( $\Gamma$ ) mode of GaSb with frequencies at  $226.7 \text{ cm}^{-1}$ ,  $231.3 \text{ cm}^{-1}$ ,  $232.4 \text{ cm}^{-1}$  for 1x1, 2x2, 3x3 SLs respectively. The weaker signal, for all cases, originates from the LO( $\Gamma$ ) mode of AlSb at  $332.4 \text{ cm}^{-1}$ ,  $335.2 \text{ cm}^{-1}$ ,  $336.8 \text{ cm}^{-1}$  for 1x1, 2x2, 3x3 SLs respectively. With increasing the layer thickness, the frequency of the LO( $\Gamma$ ) of each layer increases in order to reach the frequency of the corresponding bulk LO( $\Gamma$ ) mode. On the other hand, the increase of the layer thickness leads to stronger mode localization. This fact, in combination with the less polarizable atoms of AlSb, explains the week signals localized in the AlSb layer. Comparison of our calculations with the few experimental results, is very encouraging.

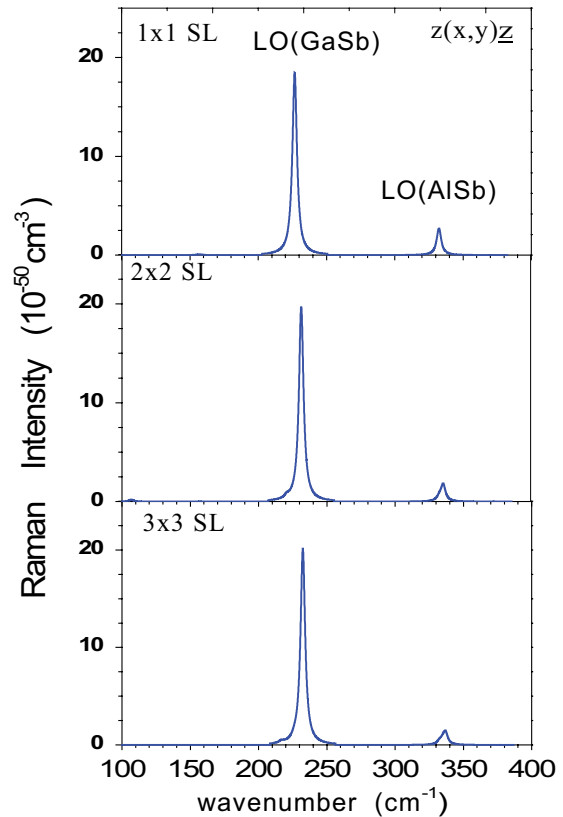


Figure 7. Raman scattering from longitudinal modes of (GaSb) $n$ /(AlSb) $n$  (001)  $n=1, 2, 3$  in the optic frequency range of the bulk constituents b/AlSb (001)

### References

1. S. G. Choi, S. K. Srivastava, C. J. Palmstrom, Y. Kim, S. L. Cooper, D. E. Aspnes, J. Vac. Sci. Tech. B23, 1149 (2005).
2. J-M. Jancu, R. Scholz, G. C. La Rocca, E. A. de Andrada, P. Voisin, Phys. Rev. B70, 121306(R) (2004).
3. G. P. Schwartz, G.J. Gualtieri, W.A. Sunder, L.A. Farrow, Phys. Rev. B36, 4868 (1987).
4. P. V. Santos, A.K. Sood, M. Cardona, K. Ploog, Y. Ohmori, H. Okamoto Phys. Rev. B37, 6381(1987).
5. G. Kanellis, W. Kress, H. Bilz, Phys. Rev. B33, 8724 (1986).
6. D. Berdekas, "Study of Lattice Dynamics of Mixed Crystals", Ph. D. Thesis (unpublished) Department of Physics, University of Thessaloniki, Thessaloniki 1991.
7. R. Tubino, L. Piseri, Phys. Rev. B11, 5145 (1975).
8. G. Kanellis, Phys. Rev. B35, 746 (1987).
9. R. A. Cowley, "The Raman Effect", p. 95, ed. A. Anderson, M. Dekker inc., New York (1971).
10. C. Flytzanis, J. Ducuing, Phys. Rev. 178, 1218 (1969).